Ligand binding promotes CDK-dependent phosphorylation of ER alpha on hinge serine 294 but inhibits ligand-independent phosphorylation of serine 305

Jason M. Held[1,5], David J. Britton[1,2,5], Gary K. Scott[1], Elbert L. Lee[1], Birgit Schilling[1], Michael A. Baldwin[1], Bradford W. Gibson[1,3], Christopher C. Benz[1,4]

Author Affiliations:
[1]The Buck Institute for Research on Aging, Novato, California 94945, USA
[2]Current Address: Proteome Sciences plc, Institute of Psychiatry, King's College, De Crespigny Park, London, SE5 8AF, UK
[3]Department of Pharmaceutical Chemistry, University of California, San Francisco, California 94143, USA
[4]Department of Medicine and Division of Oncology-Hematology, University of California, San Francisco, California 94143, USA
[5]These authors made equal contributions to this work.

Running title: Ligand binding promotes CDK-dependent phosphorylation

Keywords: Breast Cancer, Estrogen Receptor, Cyclin-Dependent Kinases, Mass Spectrometry, Multiple Reaction Monitoring

Financial Support: This work was supported by National Institutes of Health (NIH) grant, CA-R01-CA071468, a research collaboration grant from Proteome Sciences plc (UK), and Hazel P. Munroe memorial funding to the Buck Institute (C. Benz). The use of the 4000 QTRAP triple quadrupole/linear ion trap for MRM analysis was made possible by a shared instrumentation grant to the Buck Institute from the NCRR, S10 RR0021222 (B. Gibson).

To whom correspondence should be addressed:
Christopher Benz
Buck Institute for Research on Aging
8001 Redwood Blvd, Novato, CA, 94945, USA
Tel.: (415) 209-2092
Fax: (415) 209-2232
E-mail: cbenz@buckinstitute.org

ABSTRACT

Phosphorylation of estrogen receptor alpha (ERα) is critical for its transcription factor activity and may determine its predictive and therapeutic value as a biomarker for ERα positive breast cancers. Recent attention has turned to the poorly understood ERα hinge domain since phosphorylation at serine 305 (Ser305) associates with poor clinical outcome and endocrine resistance. We demonstrate that phosphorylation of a neighboring hinge domain site, Ser294, analyzed by multiple reaction monitoring mass spectrometry of ERα immunoprecipitates from human breast cancer cells is robustly phosphorylated exclusively by ligand (estradiol, tamoxifen) activation of ERα, and not by growth factor stimulation (EGF, insulin, heregulin-β). In a reciprocal fashion, Ser305 phosphorylation is induced by growth factors but not ligand activation of ERα. Phosphorylation at Ser294 and Ser305 is suppressed upon co-stimulation by EGF and ligand respectively, unlike the N-terminal (AF-1) domain Ser118 and Ser167 sites of ERα where phosphorylation is enhanced by ligand and growth factor co-stimulation. Inhibition of cyclin-dependent kinases (CDKs) by roscovitine or SNS-032 suppresses ligand-activated Ser294 phosphorylation without affecting Ser118 or Ser104/Ser106 phosphorylation. Likewise, cell-free studies using recombinant ERα and specific cyclin-CDK complexes suggest that Ser294 phosphorylation is primarily induced by the transcription-regulating and cell cycle-independent kinase CDK7. Thus, CDK-dependent phosphorylation at Ser294 differentiates ligand-dependent from ligand-independent activation of Ser305 phosphorylation, demonstrating that hinge domain phosphorylation patterns uniquely inform on the various ERα activation mechanisms thought to underlie the biological and clinical diversity of hormone-dependent breast cancers.

INTRODUCTION

As a member of the nuclear hormone receptor family, ERα plays a complex and diverse role in orchestrating such organ-specific functions as mammary gland development, bone homeostasis and cardiovascular vitality (1). The varied physiologic mechanisms driven by this sex steroid receptor are primarily initiated by its high affinity binding to an endogenous estrogenic ligand, 17-β-estradiol (E2), which triggers both non-genomic (membrane based protein interactions) and genomic (nuclear based

DNA interactions) receptor responses (2). In the context of nearly 70% of newly diagnosed human breast cancers, the full-length 67 kDa ERα protein is transcriptionally and translationally overexpressed, driving both preneoplasia as well as invasive tumor growth and metastasis (2). This key role of ERα in promoting the development and clinical progression of breast cancer explains the impressive clinical success of ligand-targeted antiestrogenic therapeutics (e.g. tamoxifen, aromatase inhibitors) in both preventing and treating ER-positive breast cancer (2).

Despite the clinical success of antiestrogenic agents, 30-50% of ER-positive breast cancers exhibit either *de novo* or acquired resistance to ligand-targeted therapeutics, yet at least 80% of these resistant tumors retain their receptor overexpression and dependence on ERα genomic and non-genomic activities (3). Understanding the molecular mechanisms promoting antiestrogen resistance and breast cancer escape from ERα ligand dependence has been challenging, leading to the emergence of receptor crosstalk as a mechanistic paradigm wherein growth factor activated cell signaling pathways converge to structurally alter ERα protein in such a way as to activate its genomic and non-genomic functions, even in the absence of ligand (3, 4). This paradigm of ligand-independent ERα activation by crosstalking signal transduction pathways extends to other members of the ligand binding hormone receptor family (5), and builds upon more than a decade of evidence that such receptors are subject to a constellation of structurally significant and functionally important post-translational modifications (PTMs) which occur throughout the receptor protein either in the presence or absence of bound ligand. With regard to ERα, phosphorylation (on serine, threonine or tyrosine residues) is the most common and best studied although ERα PTMs also include acetylation, methylation, sumoylation and ubiquitination (2). While the functional and clinical consequences of these various ERα PTMs remain largely obscure, recent identification of protein kinases linked to specific ERα phosphorylation sites, including those capable of transcriptionally activating ERα in the absence of ligand (2, 3), have stimulated interest in growth factor signaling pathways potentially associated with antiestrogen resistance mechanisms that may be therapeutically targeted by small molecule kinase inhibitors (3).

Early studies identified several serine residues in the N-terminal activation function 1 domain (AF-1) of ERα, most prominently Ser118 and Ser167, as being phosphorylated with receptor activation in ER-positive breast cancer cells exposed to ligand or growth factors (2, 6). Limited retrospective clinical studies using antibodies to interrogate ERα phosphorylation at either Ser118 or Ser167 in archived primary breast tumors with known responsiveness to tamoxifen therapy have either shown no significant response association or a surprising correlation with increased tamoxifen sensitivity (2, 6-8). However, recent attention has focused on the ERα hinge domain where phosphorylation at Ser305 appears to be correlated with antiestrogen resistance (9-12). The ERα hinge domain is a short, flexible region linking the ligand binding and activation 2 domain (LBD/AF-2) with the DNA-binding domain (DBD), and is thought to play an important role facilitating conformational synergy between the LBD/AF-2 and the AF-1 domains following ligand binding (13). Only 60 amino acids in length, the hinge domain can become highly decorated by acetylation (14), ubiquitination (15), sumoylation (16), or methylation (17) in addition to phosphorylation, suggesting that PTMs play an important regulatory role in ERα activation.

Our recent mass spectrometry screen for ERα PTMs revealed a novel hinge domain phosphorylation site at Ser294, present in E2 exposed MCF-7 cells, a human breast cancer cell line (18). While early investigations into ERα residues targeted for phosphorylation had considered Ser294 a potential candidate given its association with a proline directed kinase motif (19), more extensive studies have been hampered by the lack of facile methods to interrogate Ser294 phosphorylation. Nonetheless, very recent studies in addition to results presented here have shown that Ser294 is, in fact, phosphorylated in response to ligand and that this phosphorylation is required for full transcriptional activity by ERα (18, 20). In this report we use multiple reaction monitoring mass spectrometry (MRM/MS) to quantitatively evaluate the endogenous induction of Ser294 phosphorylation within various ER-positive breast cancer models, and show that robust Ser294 phosphorylation occurs exclusively upon ligand stimulation (E2 or tamoxifen) and not following growth factor stimulation (EGF, insulin, heregulin-β) of ERα, unlike phosphorylation occurring at Ser118,

Ser167 or Ser305. These quantitative MRM/MS findings are independently validated by immunoassay using a newly generated anti-pSer294 polyclonal antibody. Moreover, specific comparison of hinge phosphorylation at Ser294 and Ser305 reveals not only their reciprocal responsiveness to ligand-dependent vs. ligand-independent ERα activation but also their reciprocal blunting of phosphorylation upon combined ligand and growth factor stimulation, suggesting that the hinge domain acts as a specific readout for the mode of ERα activation as well as a sensor of receptor crosstalk. Lastly, treatment of cells with small molecule cyclin dependent kinase (CDK) inhibitors as well as cell-free assays using recombinant ERα and specific cyclin-CDK complexes demonstrate that the subset of transcription-regulating and cell cycle-independent kinases, most prominently CDK7, mediate ligand-dependent phosphorylation of Ser294 without affecting other ERα phosphorylation sites including Ser118, Ser104, or Ser106. This observation is made therapeutically relevant by the clinical advancement of specific inhibitors of this CDK7 subclass.

MATERIALS AND METHODS

Cell culture and reagents–The human breast cancer cell lines MCF-7, BT474, and T47D were originally obtained from American Type Culture Collection (Manassas, VA) and were grown under American Type Culture Collection-recommended conditions: 37°C, 5% CO_2, and in Dulbecco's modified Eagle's, McCoys 5A, or RPMI-1640 media, supplemented with 10% fetal bovine serum, 1% penicillin-streptomycin. (Mediatech, Inc., Herndon, VA) supplemented with 10% fetal bovine serum (Mediatech), 1% penicillin/streptomycin (Mediatech). We obtained phenol red-free Dulbecco's modified Eagle's medium supplemented with L-glutamine, and recombinant EGF and ERα from Invitrogen (Carlsbad, CA), charcoal stripped (CS) serum from Hyclone (Thermo Scientific, Pittsburgh, PA), β-Estradiol, 4-hydroxytamoxifen (TAM), okadaic acid, forskolin, insulin heregulin-β and IGEPAL CA-630 from Sigma-Aldrich (St Louis, MO), ERα antibody (clone F-10) from Santa Cruz Biotechnology (Santa Cruz, CA), pSer118 and pSer167 monoclonal antibodies from Cell Signaling (Danvers, MA), pSer104/pSer106 rabbit monoclonal antibody from Epitomics (Burlingame, CA) and pSer305 rabbit monoclonal antibody (clone 124.9.4) from Millipore (Billerica, MA).

ERα transfection assays–Full length ERα cloned into the pSG5 expression vector (gift of Paul Webb, UCSF) was used to produce wildtype ERα while expression of the Ser294Ala ERα mutant from pSG5 was obtained by replacing a unique NotI-HindIII fragment containing the Ser294 codon with the corresponding fragment containing the Ser294Ala mutation (Ser294Ala ERα mutant plasmid, gift of Susan Fuqua, Baylor College of Medicine). Both ERα wildtype and Ser294Ala mutant plasmids were verified by sequencing. To achieve approximately 3 times endogenous ERα levels, $4x10^5$ MCF-7 cells plated into 60 mm dishes were transfected with 0.5 µg of pSG5 wildtype ERα, pSG5 Ser294 mutant ERα or the empty vector pSG5 using lipofectamine 2000 from Invitrogen (Carlsbad, CA) in Dulbecco's modified Eagle's medium for 6 h. The media was then replaced with medium supplemented with 10% fetal bovine serum for an additional 18 h after which time the media was replaced with phenol red-free Dulbecco's modified Eagle's medium-H-16 supplemented with 10% charcoal stripped serum. Following 36 h in the phenol-red-free charcoal stripped serum, cells were either treated with 10 nM E2 or left untreated for an additional 6 h after which cells were harvested for total cell lysates or RNA using Trizol from Invitrogen (Carlsbad, CA). Experiments were repeated three times with each experiment using two 60 mm dishes per condition per vector.

RT-PCR quantification–Total RNA was harvested using Trizol followed by treatment with DNA-free (Ambion, Austin, TX) according to the manufacturer's specifications to remove potentially contaminating DNA. Reversed transcription was performed using oligo dT priming of 0.5 µg RNA per sample condition with SuperScript II (Invitrogen, Carlsbad, CA) according to manufacturer's specifications. PCR reactions used 1 µl aliquots from the RT reactions with Pfu polymerase (New England Biolabs, Ipswich, MA). Reaction conditions consisted of annealing at 60°C for 30 s, extension at 72°C for 25 s and denaturation at 96°C for 10 s with identically prepared reactions subjected to 24, 26 or 28 PCR cycles. PCR products were electrophoresed on 8% polyacrylamide gels, stained with eithidum bromide, photographed and quantified by densitometry using a GS-710 Calibrated Imaging Densitometer (Bio-Rad, Hercules, CA). Error bars on Figure 1B represent the standard deviation of gel

stained intensities normalized by the respective GAPDH intensity from the three separate transfection experiments. Validation of statistical difference was performed using a t-test (two-sample assuming unequal variance) with asterisks indicating significant reductions ($p<0.05$) in the Ser294Ala levels relative to E2 stimulated empty vector levels and WT ERα levels. Primers include: AREG (Amphiregulin) 170bp 5'aaaaagggaggcaaaaatgg3' (forward), 5'tcatggacttttccccaca3' (reverse); EGR3 238bp 5'gcagcatggtcttgactgaa3' (forward), 5'ccccctttccactagagtcc3' (reverse); CXCL12 221bp 5'ctagtcaagtgcgtccacga3' (forward) 5'ggacacaccacagcacaaac3' (reverse); GAPDH 234bp 5'cgaatttggctacagcaacagg3' (forward), 5'gtacatgacaaggtgcggctc3' (reverse).

Cell culture treatment conditions and ERα immunoprecipitation–24 h prior to ERα isolation, the standard cell growth media was removed, the cells washed three times with PBS (room temperature), and replaced with phenol red-free Dulbecco's modified Eagle's medium with or without 10% charcoal stripped (CS) serum depending upon treatment conditions. The various E2 and growth factor treatment regimens are detailed in appropriate Figure legends and Results section. Following treatment, the cells were washed once with room temperature PBS before harvesting on ice using a cell scraper with 1.0 ml of ice cold cell lysis buffer [100 mM NaCl, 20 mM Tris (pH 7.5), 0.5% IGEPAL-630, 100 mM NaF, 10 mM Na_3VO_4, 50 mM Na_2MoO_4, 1 tablet/10 mL PhosSTOP (Roche Applied Science, Indianapolis, IN), 320 nM okadaic acid and 1 tablet/10 mL Roche mini-complete protease inhibitor cocktail (Roche Applied Science, Indianapolis, IN)] per one 15 cm plate of cells. The cellular lysate was then sonicated twice for 10 sec while on ice and then centrifuged at 16,000 rpm (15 min, 4^{o}C). ERα from the resulting cleared supernatant was immunoprecipitated by the addition of 8 µL of ERα antibody (1.6 µg, F-10, Santa Cruz Biotechnology, Santa Cruz, CA) together with 15 µL Protein G Sepharose 4 Fast Flow beads (GE Healthcare) and incubated with slow rotation at 4°C for 6 h. The beads were then pelleted at 2500 rpm for 1 min, the supernatant was removed and the beads were washed three times in wash buffer (125 mM NaCl, 20 mM Tris pH 7.5 and 0.35% IGEPAL).

Western blot analysis–Aliquots of the immunoprecipitated ERα from the breast cancer cells were analyzed by Western blot as previously described (21). Briefly, samples were run on NuPAGE 4-

12% gels (Invitrogen), transferred to PVDF Immobilon-P membranes (Millipore) with membranes then blocked and probed using 4% nonfat dry milk power dissolved in TBST (150 mM NaCl, 50 mM Tris pH 7.5 and 0.05% Tween). Membranes were incubated with primary antibodies for 2 h at room temperature, washed in TBST then incubated with an HRP coupled secondary antibody. Washed membranes were developed using SuperSignal West Pico Chemiluminescent Substrate (Thermo Scientific).

pSer294 antibody generation–Four rabbits were immunized with a synthetic phosphopeptide corresponding to residues surrounding pSer294 of ERα according to the vendor's protocols (Epitomics, Burlingame, CA). Following immunization, the antisera were separately evaluated by Western analysis using immunoprecipitated ERα where the pSer294 levels had been previously validated by MS. The antiserum from one rabbit was particularly successful by Western analysis in recapitulating the MS results for pSer294 levels. However, as MS results consistently detect no difference, or even a slight decrease, in pSer294 levels between control and EGF stimulated ERα, the slight (~4%) increase in reactivity of this pSer294 antisera to EGF stimulated ERα versus control ERα suggest slight residual cross-reactivity to epitopes other than pSer294. Splenocytes from this rabbit are currently being used in the development of a pSer294 monoclonal antibody (Epitomic, Burlingame, CA)

On bead proteolytic digestion–To avoid electrophoretic separation and in-gel ERα digestion prior to MS, ERα immunoprecipitates were trypsin digested while complexed to the sepharose beads as previously described (18). The samples were not reduced or alkylated. Aliquots of the washed bead-bound immune complexes were transferred to siliconized 1.5 ml microcentrifuge tubes and washed twice in 100 mM Tris (pH 7.0) and three times in 25 mM NH_4HCO_3 by gentle rotation for 2 min at room temperature. 150 µL NH_4HCO_3 was added to the pelleted beads, followed by addition of 400 ng sequencing grade trypsin (23 µL of 17 ng/µL stock solution, Promega, Madison, WI), then left to incubate overnight at 37°C with shaking at 950 rpm in an Eppendorf Thermomixer. Microcentrifuge tubes were centrifuged at 12,000 rpm and the peptide solution carefully transferred (to avoid carryover of the beads) to low binding polymer technology 0.65 ml microcentrifuge tubes (PGC Scientifics,

Garner, NC). Ten µL of acetonitrile and 1 µL of 10% formic acid were added and the peptide solution was concentrated to ~15 µL. Each sample was divided into three 5 µL aliquots and stored at -80°C until used for MS.

Synthesis of stable isotope labeled SER167 and SER294 peptides–Stable isotope-labeled and -unlabeled peptides corresponding to the unmodified and phosphorylated tryptic peptides quantified by MRM for Ser167 and Ser294 were synthesized by Cambridge Peptides Ltd using Fmoc solid phase peptide chemistry and purified using reverse phase HPLC. Peptides were purified to 90 - 98% purity, each resulting in 2-3 mg of lyophilized peptide. The peptide sequences and isotope information are listed in Table 1.

Each peptide was solubilized using 5% acetonitrile, 0.1% formic acid in a volume resulting in peptide concentrations of approximately 1mM. Peptides were divided into 100 µL aliquots and stored at -80°C. One aliquot was shipped on dry ice for amino acid analysis to accurately determine the peptide concentrations. Amino acid analysis was performed at the Protein & Nucleic Acid Chemistry Facility (PNAC), Department of Biochemistry, University of Cambridge, UK. Peptides were then diluted to suitable concentrations according to the instrument parameter optimization experiments (10 pmol/µL; direct infusion), calibration curves (0.005 to 50 fmol/µL), internal standards of ER IP/digests (5 fmol/µL).

NanoLC-MRM/MS analysis–To quantify relative changes in ERα Ser167 and Ser294 phosphorylation levels by MRM/MS, ERα immunoprecipitates were analyzed by nanoLC-MRM/MS on a 4000 QTRAP hybrid triple quadrupole/linear ion trap mass spectrometer (AB Sciex, Framingham, MA) as previously described (18) and further detailed in the supplementary methods. To compare the relative levels of phosphorylated Ser294 and Ser167 in different samples, the MRM peak area of the phosphorylated peptide was divided by the unmodified peptide peak area for normalization to total ERα levels and is referred to as the “phosphorylated:unmodified peptide area ratio”. S-lens and Q2 collision energy optimization for the TSQ Vantage are described in the supplementary methods.

Stable isotope dilution MRM (SID-MRM) assay for absolute quantification of endogenous ERα tryptic peptides–To determine the molar amount of endogenous ERα by SID-MRM, following

immunoprecipitation of ER and on-bead digestion, the peptide solution was removed from the beads and 10 µL of 50% acetonitrile, 5% formic acid was added. Samples were dried in a Speedvac and re-solubilized in 25 µL of 3% acetonitrile, 0.2% formic acid containing 5 fmol/µL of each stable isotope-labeled peptide, in addition to 200 µg/mL glucagon to improve peptide stability. An 8 µL aliquot of each sample was analyzed per injection on a TSQ Vantage with detailed LC-MS instrument settings listed in the supplementary methods

Normal response curves – A response curve was generated for each peptide to determine assay characteristics including the linear range of the assay, limits of detection (LOD), and limits of quantification (LOQ). The supplementary methods section describes how the peptide response curves were generated. The LOD was calculated from the variance of the blank sample with no peptides spiked in and the variance of the lowest spiked in concentration (Lowest values shown in the table in supplementary methods) as previously described (22). Assuming a type I error rate $\alpha = 0.05$ for deciding that the peptide is present when it is not, and a type II error rate $\beta = 0.05$ for not detecting the peptide when it is present, LOD was calculated with:

$$LOD = mean_b + t_{1-\beta} * (s.d._b + s.d._S) / 2$$

Where the $t_{1-\beta}$ term is equal to the (1–β) percentile of the standard t distribution on n degrees of freedom, where n is equal to the number of replicates. LOD values were then transformed and calculated into concentrations using the linear regressions described above. This method relies on the LOD being in a region of the regression where the response is still linear. Once the LOD was determined, the LOQ was calculated using the customary relation of LOQ = 3 * LOD.

In vitro cyclin-dependent kinase assays–5 picomoles of recombinant ERα was incubated with 200 ng of the indicated cyclin-dependent kinase (SignalChem, Richmond, British Columbia) at 30ºC for 60 min in 10 mM $MgCl_2$, 60 mM HEPES pH 7.4, 1.2 mM DTT, and 100 µM ATP with a total reaction volume of 30 µL. CDK/cyclin pairs used were: CDK1/CyclinA1, CDK2/CyclinA2, CDK4/CyclinD1,

CDK7/CyclinH1/MNAT1, CDK9/CyclinK. Aliquots were then analyzed for pSer294 by western blotting or MRM/MS.

RESULTS

Functional analysis of Ser294 phosphorylation using a dominant-negative strategy–As a previous study had demonstrated the requirement of Ser294 phosphorylation to drive ERα transcriptional activity in an ERα-null cell line (20), a dominate-negative strategy was used to determine the functional relevance of pSer294 to ERα transcriptional activity in the context of an ERα positive cell line. Thus MCF-7 cells were transiently transfected with an ERα expression construct containing a Ser294Ala mutation. As a control, MCF-7 cells were transiently transfected with a wildtype ERα expression construct or empty vector (pSG5). The level of exogenous ERα introduced into the MCF-7 cells by the mutant and wild type expression constructs was approximately 3-fold above endogenous (empty-vector) ERα levels as determined by densitometry of Western blots (Figure 1A). Following 6 h of stimulation with E2 we observed the anticipated downregulation of ER protein (2.5-3 fold) in all conditions which is consistent with normal proteasomal degradation of ERα following its E2-induced transcriptional activation (Figure 1A, and (23)). To evaluate the influence of the Ser294Ala mutated ERα upon E2-dependent gene transcription we used semi-quantitative RT-PCR to measure the induction of three genes (amphiregulin, AREG; early growth response 3, EGR3; and chemokine ligand 12, CXCL12) previously known to be highly E2 inducible in MCF-7 cells following 8 h of E2 stimulation (24, 25). As seen in Figure 1B, all three of these genes showed significantly reduced (30-50%) E2 induction in the Ser294Ala ERα overexpressing MCF-7 cells relative to MCF-7 cells transfected with either wildtype ERα or empty vector ($p<0.05$). These results imply that full transcriptional activation of ERα is dependent upon pSer294.

Phosphorylation of ERα on Ser294 is not promoted by growth factors–While our previous MS study focused on detection of ERα residues phosphorylated in response to E2, the influence of growth

factors such as EGF upon ERα phosphorylation has never been investigated (18). To determine the status of Ser294 following growth factor stimulation, an optimized approach of on-bead trypsin digestion of ERα immunopurified from growth factor treated MCF-7 cells followed by MRM/MS analysis was used. Quantitative assessment of relative changes in phosphorylation status was performed by comparing the "phosphorylated:unmodified peptide area ratio", the ratio of the MRM peak area of a phosphorylated peptide normalized to the peak area of its unmodified counterpart peptide. As a positive control we analyzed ERα immunopurified from E2 treated as well as EGF treated MCF-7 cells in a multiplexed MRM/MS assay which included quantitation of Ser167 phosphorylation as an internal control to confirm that our MRM/MS method could recapitulate the induction of Ser167 phosphorylation as determined by Western analysis using a well validated pSer167 antibody. As the MRM/MS data shown in Figure 2A and summarized graphically in Figure 2B exhibits, treatment of serum starved (NS) MCF-7 cells with EGF failed to provoke any detectable induction of Ser294 phosphorylation relative to control (Figures 2A, top right panel and Figure 2B, left bar graph) while MRM/MS assessment of pSer167 within the same analysis revealed an 11-fold EGF induction of phosphorylation (Figure 2A, bottom right panel and Figure 2B, right bar graph). The latter induction of pSer167 by EGF is a result consistent with numerous previous pSer167 antibody studies (26) and was confirmed by Western analysis of the immunopurified ERα (Figure 2C). The 11-fold induction in pSer294 following E2 treatment (Figure 2A, top left panel and Figure 2B, left bar graph) and 3.2 fold E2 inductions of pSer167 (Figure 2A, bottom left panel, Figure 2B, right bar graph) in MCF-7 cells grown in charcoal stripped (CS) media are consistent with previously reported results and confirm the validity of the MRM/MS analysis (27). Two additional growth factors, insulin and heregulin-β, also failed to induce pSer294 but did upregulate pSer167 (Supplemental Figure 1), underscoring the inability of growth factors to stimulate pSer294.

Stable isotope dilution multiple reaction monitoring (SID-MRM)–To determine the phosphorylation occupancy level of both Ser167 and Ser294 we synthesized four heavy-isotope labeled peptides corresponding to the unmodified and phosphorylated forms of the Ser167 and Ser294

peptides. First, a standard curve was prepared and analyzed for each synthetic peptide (Supplemental Figure 2A) to assess the linearity of response, LOD), and LOQ (Supplemental Figure 2B) as described in the Experimental Procedures. The LOQs were determined to range between 259 and 667 attomoles (on column) for the four peptides (Supplemental Figure 2B). To determine the level of unmodified and phosphorylated Ser294 and Ser167 in MCF-7 cells using SID-MRM we spiked in 25 fmol of each of the four synthetic, heavy-isotope labeled peptides after on bead trypsin digestion of the immunopurified ERα. Since the immunoprecipitation procedure captures >98% of ERα (18) it is suitable for quantitative evaluation of absolute levels of ERα. Using this approach it was determined that the total amount of ERα per 10^6 cells of MCF-7 is 26±5 (mean±s.d.) femtomoles based on the Ser294 peptide and 16±6 femtomoles based on the Ser167 peptide (Supplemental Figure 2C) in untreated, serum-starved conditions. To determine the phosphorylation stoichiometry, or percent phosphorylation, of Ser294 and Ser167 we divided the molar amount of phosphorylated Ser167- or Ser294-containing peptide by the total amount of ERα (modified and unmodified). Under conditions of maximal phosphorylation, Ser294 was found to be 4% phosphorylated by E2 while Ser167 was 34% phosphorylated by EGF (Figure 2D).

To confirm that Ser294 is more generally induced by E2 but not EGF in multiple breast cancer model systems, two other ERα positive human breast cancer cell lines, BT474 and T47D, were analyzed in parallel with MCF-7. As shown in Figure 3A, relative quantitation by MRM/MS of ERα immunopurified from these cells lines following EGF treatment revealed no induction of pSer294. In contrast, pSer294 was induced by E2 and, to a lesser extent, by 4-hydroxytamoxifen (TAM) treatment (Figure 3B).

Differential regulation of phosphorylation at ERα Ser294 and Ser305 by growth factors and E2– As Ser294 is situated in the hinge region of ERα, it was of interest to examine the phosphorylation status of the neighboring hinge region Ser305, as phosphorylation at this serine has been implicated as a breast cancer marker indicative of poor prognosis and resistance to tamoxifen (10, 11). While detection of peptides containing residue Ser305 by MS has proven difficult (18), the recent availability of a monoclonal antibody to pSer305, which has supplanted the relatively ineffective pSer305

polyclonal antibodies, allowed for the quantitative determination of pSer305 by Western analysis on immunoprecipitated ERα. In addition, prompted by our initial MS findings on the selective induction of pSer294, we initiated development of an antibody specific for ERα pSer294 in order to independently validate our MS findings (Figure 4A). To establish that Ser305 phosphorylation was preserved in the immunopurified ERα preparations, MCF-7 cells were treated with the protein kinase A (PKA) activator forskolin, as Ser305 phosphorylation has been reported to be directly mediated by PKA with forskolin stimulation of pSer305 in MCF-7 cells successfully validated using the pSer305 monoclonal antibody (10). As shown in Figure 4A, pSer305 was induced by forskolin as well as by EGF but exhibited no induction following E2 stimulation; as expected pSer294 was only induced by E2. Furthermore, while pSer118 and pSer167 were induced by EGF as expected, they were not induced by forskolin (Figure 4A). We note that the results shown here demonstrating the inability of E2 to induce pSer305 contradicts several reports where pSer305 was detected following E2 stimulation in whole cell lysates using a pSer305 polyclonal antibody (28, 29)

Given the diametrically opposing influences of E2 and growth factors in promoting pSer294 and pSer305, the consequence of co-stimulating with E2 and EGF were examined. Treating MCF-7 cells that had been serum starved for 24 h with a 20 min stimulation of EGF, E2, or co-administration of both E2 and EGF (8 nM EGF, 10 nM E2) indicated that while Ser294 phosphorylation was slightly blunted by the EGF and E2 combination relative to E2 alone, induction of pSer305 by EGF was dramatically suppressed by co-stimulation with E2 (Figure 4B). In response to decreasing doses of E2 (10 nM, 2 nM, or 0.2 nM E2) in combination with 8 nM EGF, a reciprocal dose-response was observed with a reduction in pSer294 levels accompanied by increased pSER305 levels (Figure 4B) In contrast, the robust EGF stimulation of pSer167, enhanced by E2 co-stimulation, remained relatively unaltered across the E2 titration spectrum (Figure 4B). MRM/MS analysis of pSer294 and pSer167 confirmed these Western results with E2 and EGF co-treatment producing a 32% suppression of Ser294 phosphorylation and a 70% phosphorylation increase in pSer167 induction compared to any signal agent treatment (Figure 4C).

Cyclin-dependent kinases (CDKs) phosphorylate ERα at Ser294–Because of the central role played by ERα in mediating many key signaling pathways, there has been considerable effort to determine the kinases promoting the site- and stimuli-specific phosphorylation of ERα (2, 26). With Ser294 positioned between two prolines (Pro-Ser-Pro), the kinase predictors Scansite (30) and NetPhosK (31) identified Ser294 as a potential CDK site. To test if CDKs are capable of directly phosphorylating Ser294 we first performed an *in vitro* kinase assay using recombinant CDKs 2, 4, 7 and 9 with recombinant ERα as substrate. As shown in Figure 5A, pSer294 is phosphorylated maximally by CDK7 and to a lesser extent by CDKs 2, 4 and 9.

Having established that Ser294 was targeted by CDKs in vitro, the influence of CDKs upon pSer294 formation in MCF-7 cells was examined pharmacologically using a variety of well established, CDK-selective small molecule inhibitors as opposed to CDK siRNA approaches, since CDK protein downregulation can produce more complex phenotypic changes confounding experimental interpretation (19). Following 1 h pretreatment of MCF-7 cells with the different CDK small molecule inhibitors, cells where E2 stimulated for an additional 30 min before ERα harvesting. As shown in Figure 5B, pretreatment with the pan-CDK inhibitor, roscovitine at 50 uM and 5uM, as well as pretreatment with the more selective CDK inhibitor SNS-032 (CDK 2, 7, and 9 (32)) at a low dose of 1 uM suppressed E2 induction of pSer294 by approximately 89% following roscovitine pretreatments and 52% following SNS-032 pretreatment relative to E2 treatment alone, as determined by MRM/MS analysis of immunopurified ERα. As roscovitine treatment had previously been used to demonstrate that E2 induction of pSer118 was not CDK mediated (33), Western analysis was used to confirm that the CDK inhibitor treatments did not influence E2 induction of pSer118 as well as to validate the MRM/MS result for CDK inhibitor suppression of pSer294 induced by E2 (Figure 5C). Additionally, the availability of a rabbit monoclonal antibody to ERα pSer104/pSer106, two other AF-1 domain serines putatively targeted by CDKs (34), allowed examination of the CDK responsiveness of these sites. As shown in Figure 5C, CDK inhibition produced no change in the slightly enhanced (vs. control) level of

E2 induced pSer104/pSer106. These results strongly argue that, following E2 stimulation, Ser294 is the primary CDK target on intracellular ERα among known phosphorylation sites.

DISCUSSION

The constellation of phosphorylated residues within the endogenous ERα of human breast cancers, that functionally direct receptor conformation, protein-protein interactions and genomic activity, also represent a post-translational code reflecting the integration of ligand-dependent and ligand-independent ERα activation signals (2, 6). Up to 50% of ER-positive breast cancers exhibit endocrine resistance to ligand-targeted therapeutics, yet retain some dependence on the growth promoting genomic (+/- non-genomic) activity of activated ERα. As a result, clinical investigators continue to evaluate the combination of standard endocrine agents with various small molecule inhibitors of protein kinase crosstalking pathways presumed to target ERα and drive the ligand-independent growth and endocrine resistance of ER-positive breast cancers (3, 4). Despite compelling pre-clinical rationale for these therapeutic combinations, these clinical trials have been inconclusive due to the lack of validated biomarkers, other than the presence of ERα itself, which have the ability to predict endocrine sensitivity or point to specific protein kinases targeting ERα that may induce endocrine resistance. Ser118 and Ser167 were identified early on as AF-1 domain phosphorylation sites linked to ERα genomic activity and responsive to a multitude of different signaling kinases (2, 6). The clinical expectation was that phosphorylation at one or both of these AF-1 sites would identify endocrine-resistant breast cancers. However, the null or even opposite clinical findings correlating Ser118 and Ser167 phosphorylation with endocrine responsiveness (6-8) may now be understood in the light of the present study, which compares ERα hinge and AF-1 domain phosphorylation responses in ER-positive breast cancer cells exposed to ligands, growth factors, or a combination of ligand-dependent and ligand-independent cell stimuli. From these findings it is clear that either ER ligands or growth factors can induce AF-1 (Ser118, Ser167) phosphorylation, and that this phosphorylation is enhanced by the combination of these ERα stimuli compared to either stimulus alone. Thus, it is mechanistically unlikely that Ser118 or Ser167

phosphorylation status can discriminate between ligand-dependent and ligand-independent ERα activation let alone point to specific protein kinases involved in ligand-independent receptor crosstalk. In contrast, as we demonstrate here, the phosphorylation status of neighboring hinge domain sites at Ser294 and Ser305 is capable of differentiating between ligand-dependent and ligand-independent ERα activation.

Hinge domain phosphorylation at Ser305 was found within the past decade to be linked to two different protein kinases in an apparent ligand-independent manner (9, 10). The recent development of a monoclonal antibody specific to phosphorylated Ser305 enabled initial breast cancer biomarker studies to claim that ERα phosphorylation at this site may correlate with antiestrogen resistance (11, 12). About this same time, and using an MRM/MS approach, we first identified the presence of another hinge domain phosphorylation site at Ser294 expressed in ligand (E2) stimulated MCF-7 cells (18). As illustrated here using a quantitative MRM/MS approach, ERα phosphorylation at Ser294 occurs in a variety of breast cancer cell lines (MCF-7, T47D, BT474) following E2 stimulation. The fact that a partially agonistic ligand like TAM is also capable of inducing pSer294, but to a lesser extent than the fully agonistic E2 ligand, indicates that this hinge phosphorylation response does not depend on a specific change in ERα helix 12 conformation within the C-terminal ligand binding domain. During the course of our MRM/MS studies, we developed a polyclonal rabbit antisera capable of specifically detecting ERα phosphorylation at Ser294 in ERα immunoprecipitated samples, enabling independent validation of our MRM/MS results by western blotting. Using both MRM/MS and immunoblotting approaches, we evaluated immunoprecipitated ERα from cells exposed to various growth factor (EGF, insulin, heregulin-β) stimuli, finding none that could induce Ser294 phosphorylation although they were fully capable of inducing phosphorylation at Ser118 and Ser167 in the AF-1 domain and at the neighboring hinge Ser305 site. Therefore, the unique ability of Ser294 to respond only to ligand stimuli sets it apart from all other known ERα phosphorylation sites and enables it to serve as a specific readout for ligand-dependent ERα activation. Additionally, the dominant negative experiments shown in Figure 1 using an ERα expression construct mutated at Ser294 reinforces previous results (20)

suggesting that phosphorylation at Ser294 is required for ERα to promote full ligand induced transcriptional activity.

To test the utility of using both Ser294 and Ser305 phosphorylation as companion readouts to distinguish ligand-dependent from ligand-independent ERα activation, we co-stimulated cells with EGF (8 nM) and varying physiological concentrations of E2 (0.2, 2.0, 10 nM), and then compared the hinge phosphorylation responses to those produced by ligand or growth factor stimulation alone. While EGF appeared to blunt E2 induced Ser294 phosphorylation by ≤20% compared to E2 alone, increasing doses of E2 caused progressively greater suppression of EGF induced Ser305 phosphorylation, reaching more than 98% suppression at 10 nM E2 relative to EGF alone. Since cell exposure to 10 nM E2 or 8 nM EGF maximally stimulated Ser294 and Ser305 phosphorylation respectively, the mild suppression of Ser294 phosphorylation by EGF and the profound suppression of Ser305 phosphorylation by E2 are not simply consequences of inadequate receptor stimulation by either ligand or growth factor. It is also noteworthy that when using the CDK inhibitor roscovitine to suppress E2 induced Ser294 phosphorylation, the corresponding E2 induced suppression of Ser305 phosphorylation was abated relative E2 alone (data not shown). While future studies are needed to understand what enzymatic or protein-protein interactions mediate the apparent mutual exclusivity of phosphorylation events at neighboring Ser294 and Ser305 sites, these findings reinforce the conclusion that phosphorylation at these two hinge sites may be useful readouts to discriminate between ligand-dependent and ligand-independent ERα activation respectively.

Identification of the kinase mediating E2 induction of pSer294 was of considerable interest both to expand understanding of ERα function as well as to provide future rationale for combining kinase inhibitors with endocrine therapeutics. Ser294 was the only one of four sites in ERα harboring a proline directed kinase motif (Ser-Pro), for which the kinase responsible for phosphorylation remained unknown (2). Using a broadly active CDK inhibitor roscovitine, or a more selective CDK inhibitor, SNS-032, that targets CDKs 2, 7 and 9 (35), the E2 induction of pSer294 was suppressed by ~80% and 50% respectively relative to E2 stimulation alone. In contrast, simultaneous interrogation of other AF-1

phosphorylation sites confirmed an earlier report that E2 induction of pSer118 phosphorylation cannot be suppressed by roscovitine (33). Moreover, induction of Ser104 and Ser106 phosphorylation, two other potential CDK sites (34), was not inhibited by roscovitine. Therefore, Ser294 stands as the only CDK-mediated ERα phosphorylation site and, as such, likely plays a key role in the roscovitine-induced suppression of proliferation observed in tamoxifen-resistant breast cancer cells (36).

As our quantitative MRM/MS analyses indicated that nearly 5% of ERα is marked by Ser294 phosphorylation upon E2 binding and activation, it is noteworthy that this compares with the estimated amount of chromatin-bound ERα induced upon ligand stimulation of MCF-7 cells (37). Chromatin immunoprecipitation (CHIP) experiments have documented the ligand-dependent recruitment of ERα to gene promoters in conjunction with TFIID, a multi-protein transcription factor complex known to contain CDK7 (35, 37). In this regard, it is worthy of note that our CDK *in vitro* kinase assay clearly showed CDK7 as the CDK family member capable of promoting the most robust phosphorylation of ERα on Ser294. Along with the fact that our cellular E2 induction of Ser294 phosphorylation was measured under serum-free culture conditions in which the MCF-7 breast cancer cells are viable and transcribing but not actively dividing, these kinase studies lead us to conclude that ligand induced endogenous phosphorylation of Ser294 is mediated primarily by the transcription-regulating and cell cycle-independent kinase, CDK7, a therapeutic target of current clinical interest whose expression appears to be significantly upregulated in breast cancers relative to matched normal breast tissues (GSE15852; 38).

In conclusion, key results are summarized schematically in the model diagram shown in Figure 6. Here, hinge domain phosphorylations at Ser294 and Ser305 are represented as mutually exclusive ERα states, functionally distinct from AF-1 phosphorylation responses where both Ser118 and Ser167 phosphorylations are stimulated by ligand and growth factor treatment. Phosphorylation at Ser294 predominates upon ligand induced receptor activation with this phosphorylation state becoming partially blunted by growth factor co-treatment. In contrast, phosphorylation at Ser305 is maximal under conditions of growth factor stimulation (crosstalk) but becomes rapidly suppressed as estrogen

concentrations are raised. As inferred from the western blot of Figure 4B, with estrogen and EGF concentrations at their standard 10 nM and 8 nM levels respectively, co-treatment produces at least 50-fold suppression of pSer305 levels relative to the EGF condition while pSer294 levels are suppressed by less than ~10%. However, translating results from an *in vitro* model system into relevant *in vivo* clinical situations remains a challenge particularly when trying to understand how the various constellations of ERα phosphorylations might predict ERα positive breast cancer outcome and responsiveness to antiestrogenic therapy. In addition to a series of clinical studies using phospho-specific antibodies to evaluate pSer118, pSer167 and pSer305 as single markers of endocrine responsiveness (39), another report has shown significantly better outcome predictability when multiple phospho-specific antibodies directed against a suite of phosphorylated ERα sites (including those not shown in Figure 6) are employed (39, 40). While pSer294 was among the seven different ERα phosphorylation sites evaluated in this latter analysis of over 300 tamoxifen treated breast cancer cases, unfortunately, pSer305 was not evaluated (40). The recent commercial availability of a pSer305 antibody and our current development of a more robust rabbit monoclonal directed at ERα pSer294 offer a future opportunity to demonstrate that hinge phosphorylation at Ser294 and Ser305 may be sufficient to discriminate endocrine-sensitive from endocrine-resistant breast cancers. It is also possible that rapidly evolving mass spectrometry technologies will provide even greater clinical predictive power over standard IHC or other antibody-based ERα assays. While the sensitivity of antibodies to interrogate thin slices of fixed tissue for a single epitope would be difficult to match using current mass spectrometry methods, the ability of mass spectrometry to perform global proteomic analysis and to interrogate the stoichiometry of ERα phosphorylation at either one specific residue of interest or across multiple phosphorylation sites within the same ERα peptide region offer better PTM definition and potentially improved clinical predictive utility over that achievable by any current immunoassays. .

ACKNOWLEGMENTS

We would like to thank Christina Yau for bioinformatic advice.

GRANT SUPPORT

This work was supported by National Institutes of Health (NIH) grant R01-CA071468, a research collaboration grant from Proteome Sciences plc (UK), and Hazel P. Munroe memorial funding to the Buck Institute (C. Benz). The use of the 4000 QTRAP triple quadrupole/linear ion trap for MRM analysis was made possible by a shared instrumentation grant to the Buck Institute from the NCRR, S10 RR0021222 (B. Gibson).

REFERENCES

1. Deroo BJ, Korach KS. Estrogen receptors and human disease. The Journal of clinical investigation. 2006;116:561-70.
2. Le Romancer M, Poulard C, Cohen P, Sentis S, Renoir JM, Corbo L. Cracking the estrogen receptor's posttranslational code in breast tumors. Endocrine reviews. 2011;32:597-622.
3. Osborne CK, Schiff R. Mechanisms of endocrine resistance in breast cancer. Annual review of medicine. 2011;62:233-47.
4. Miller TW, Balko JM, Arteaga CL. Phosphatidylinositol 3-kinase and antiestrogen resistance in breast cancer. Journal of clinical oncology : official journal of the American Society of Clinical Oncology. 2011;29:4452-61.
5. Weigel NL, Moore NL. Steroid receptor phosphorylation: a key modulator of multiple receptor functions. Mol Endocrinol. 2007;21:2311-9.
6. Murphy LC, Seekallu SV, Watson PH. Clinical significance of estrogen receptor phosphorylation. Endocrine-related cancer. 2011;18:R1-14.
7. Jiang J, Sarwar N, Peston D, Kulinskaya E, Shousha S, Coombes RC, et al. Phosphorylation of estrogen receptor-alpha at Ser167 is indicative of longer disease-free and overall survival in breast cancer patients. Clinical cancer research : an official journal of the American Association for Cancer Research. 2007;13:5769-76.
8. Murphy LC, Skliris GP, Rowan BG, Al-Dhaheri M, Williams C, Penner C, et al. The relevance of phosphorylated forms of estrogen receptor in human breast cancer in vivo. The Journal of steroid biochemistry and molecular biology. 2009;114:90-5.
9. Wang RA, Mazumdar A, Vadlamudi RK, Kumar R. P21-activated kinase-1 phosphorylates and transactivates estrogen receptor-alpha and promotes hyperplasia in mammary epithelium. The EMBO journal. 2002;21:5437-47.
10. Michalides R, Griekspoor A, Balkenende A, Verwoerd D, Janssen L, Jalink K, et al. Tamoxifen resistance by a conformational arrest of the estrogen receptor alpha after PKA activation in breast cancer. Cancer cell. 2004;5:597-605.
11. Holm C, Kok M, Michalides R, Fles R, Koornstra RH, Wesseling J, et al. Phosphorylation of the oestrogen receptor alpha at serine 305 and prediction of tamoxifen resistance in breast cancer. The Journal of pathology. 2009;217:372-9.

12. Kok M, Zwart W, Holm C, Fles R, Hauptmann M, Van't Veer LJ, et al. PKA-induced phosphorylation of ERalpha at serine 305 and high PAK1 levels is associated with sensitivity to tamoxifen in ER-positive breast cancer. Breast cancer research and treatment. 2011;125:1-12.
13. Zwart W, de Leeuw R, Rondaij M, Neefjes J, Mancini MA, Michalides R. The hinge region of the human estrogen receptor determines functional synergy between AF-1 and AF-2 in the quantitative response to estradiol and tamoxifen. Journal of cell science. 2010;123:1253-61.
14. Wang C, Fu M, Angeletti RH, Siconolfi-Baez L, Reutens AT, Albanese C, et al. Direct acetylation of the estrogen receptor alpha hinge region by p300 regulates transactivation and hormone sensitivity. The Journal of biological chemistry. 2001;276:18375-83.
15. Berry NB, Fan M, Nephew KP. Estrogen receptor-alpha hinge-region lysines 302 and 303 regulate receptor degradation by the proteasome. Mol Endocrinol. 2008;22:1535-51.
16. Sentis S, Le Romancer M, Bianchin C, Rostan MC, Corbo L. Sumoylation of the estrogen receptor alpha hinge region regulates its transcriptional activity. Mol Endocrinol. 2005;19:2671-84.
17. Subramanian K, Jia D, Kapoor-Vazirani P, Powell DR, Collins RE, Sharma D, et al. Regulation of estrogen receptor alpha by the SET7 lysine methyltransferase. Molecular cell. 2008;30:336-47.
18. Atsriku C, Britton DJ, Held JM, Schilling B, Scott GK, Gibson BW, et al. Systematic mapping of posttranslational modifications in human estrogen receptor-alpha with emphasis on novel phosphorylation sites. Molecular & cellular proteomics : MCP. 2009;8:467-80.
19. Le Goff P, Montano MM, Schodin DJ, Katzenellenbogen BS. Phosphorylation of the human estrogen receptor. Identification of hormone-regulated sites and examination of their influence on transcriptional activity. The Journal of biological chemistry. 1994;269:4458-66.
20. Williams CC, Basu A, El-Gharbawy A, Carrier LM, Smith CL, Rowan BG. Identification of four novel phosphorylation sites in estrogen receptor alpha: impact on receptor-dependent gene expression and phosphorylation by protein kinase CK2. BMC biochemistry. 2009;10:36.
21. Scott GK, Marx C, Berger CE, Saunders LR, Verdin E, Schafer S, et al. Destabilization of ERBB2 transcripts by targeting 3' untranslated region messenger RNA associated HuR and histone deacetylase-6. Molecular cancer research : MCR. 2008;6:1250-8.
22. Addona TA, Abbatiello SE, Schilling B, Skates SJ, Mani DR, Bunk DM, et al. Multi-site assessment of the precision and reproducibility of multiple reaction monitoring-based measurements of proteins in plasma. Nature biotechnology. 2009;27:633-41.
23. Nawaz Z, Lonard DM, Dennis AP, Smith CL, O'Malley BW. Proteasome-dependent degradation of the human estrogen receptor. Proceedings of the National Academy of Sciences of the United States of America. 1999;96:1858-62.
24. Creighton CJ, Cordero KE, Larios JM, Miller RS, Johnson MD, Chinnaiyan AM, et al. Genes regulated by estrogen in breast tumor cells in vitro are similarly regulated in vivo in tumor xenografts and human breast tumors. Genome Biol. 2006;7:R28.
25. Britton DJ, Hutcheson IR, Knowlden JM, Barrow D, Giles M, McClelland RA, et al. Bidirectional cross talk between ERalpha and EGFR signalling pathways regulates tamoxifen-resistant growth. Breast cancer research and treatment. 2006;96:131-46.
26. Lannigan DA. Estrogen receptor phosphorylation. Steroids. 2003;68:1-9.
27. Britton DJ, Scott GK, Schilling B, Atsriku C, Held JM, Gibson BW, et al. A novel serine phosphorylation site detected in the N-terminal domain of estrogen receptor isolated from human breast cancer cells. Journal of the American Society for Mass Spectrometry. 2008;19:729-40.
28. Al-Dhaheri MH, Rowan BG. Protein kinase A exhibits selective modulation of estradiol-dependent transcription in breast cancer cells that is associated with decreased ligand binding,

altered estrogen receptor alpha promoter interaction, and changes in receptor phosphorylation. Mol Endocrinol. 2007;21:439-56.
29. Giordano C, Cui Y, Barone I, Ando S, Mancini MA, Berno V, et al. Growth factor-induced resistance to tamoxifen is associated with a mutation of estrogen receptor alpha and its phosphorylation at serine 305. Breast cancer research and treatment. 2010;119:71-85.
30. Obenauer JC, Cantley LC, Yaffe MB. Scansite 2.0: Proteome-wide prediction of cell signaling interactions using short sequence motifs. Nucleic acids research. 2003;31:3635-41.
31. Blom N, Sicheritz-Ponten T, Gupta R, Gammeltoft S, Brunak S. Prediction of post-translational glycosylation and phosphorylation of proteins from the amino acid sequence. Proteomics. 2004;4:1633-49.
32. Chen R, Wierda WG, Chubb S, Hawtin RE, Fox JA, Keating MJ, et al. Mechanism of action of SNS-032, a novel cyclin-dependent kinase inhibitor, in chronic lymphocytic leukemia. Blood. 2009;113:4637-45.
33. Weitsman GE, Li L, Skliris GP, Davie JR, Ung K, Niu Y, et al. Estrogen receptor-alpha phosphorylated at Ser118 is present at the promoters of estrogen-regulated genes and is not altered due to HER-2 overexpression. Cancer research. 2006;66:10162-70.
34. Rogatsky I, Trowbridge JM, Garabedian MJ. Potentiation of human estrogen receptor alpha transcriptional activation through phosphorylation of serines 104 and 106 by the cyclin A-CDK2 complex. The Journal of biological chemistry. 1999;274:22296-302.
35. Lapenna S, Giordano A. Cell cycle kinases as therapeutic targets for cancer. Nature reviews Drug discovery. 2009;8:547-66.
36. Nair BC, Vallabhaneni S, Tekmal RR, Vadlamudi RK. Roscovitine confers tumor suppressive effect on therapy-resistant breast tumor cells. Breast cancer research : BCR. 2011;13:R80.
37. Welboren WJ, van Driel MA, Janssen-Megens EM, van Heeringen SJ, Sweep FC, Span PN, et al. ChIP-Seq of ERalpha and RNA polymerase II defines genes differentially responding to ligands. The EMBO journal. 2009;28:1418-28.
38. Wesierska-Gadek J, Kramer MP. The impact of multi-targeted cyclin-dependent kinase inhibition in breast cancer cells: clinical implications. Expert opinion on investigational drugs. 2011;20:1611-28.
39. Skliris GP, Nugent ZJ, Rowan BG, Penner CR, Watson PH, Murphy LC. A phosphorylation code for oestrogen receptor-alpha predicts clinical outcome to endocrine therapy in breast cancer. Endocrine-related cancer. 2010;17:589-97.
40. Skliris GP, Rowan BG, Al-Dhaheri M, Williams C, Troup S, Begic S, et al. Immunohistochemical validation of multiple phospho-specific epitopes for estrogen receptor alpha (ERalpha) in tissue microarrays of ERalpha positive human breast carcinomas. Breast cancer research and treatment. 2009;118:443-53.

TABLES

TABLE 1. Stable isotope labeled-peptides synthesized

Peptide Name	Amino Acid Sequence	Stable Isotope label
Heavy SER167	LASTNDKGSMAMESAK	K, U-13C6; 15N2
Light SER167	LASTNDKGSMAMESAK	
Heavy pSER167	LASTNDKGSMAMESAK	K, U-13C6; 15N2
Light pSER167	LASTNDKGSMAMESAK	
Heavy SER294	AANLWPSPLMIK	K, U-13C6; 15N2
Light SER294	AANLWPSPLMIK	
Heavy pSER294	AANLWPSPLMIK	K, U-13C6; 15N2
Light pSER294	AANLWPSPLMIK	

Table of the synthetic stable isotope-labeled and -unlabeled peptides used to generate a calibration curve and measure absolute levels of phosphorylated and unmodified Ser167 and Ser294 of ERα with a stable isotope dilution multiple reaction monitoring (SID-MRM) assay. The underlined K indicates the position of the heavy labeled lysine and the underlined S indicates the phosphorylation site in each peptide.

FIGURES

FIGURE 1. MCF-7 cells transfected with a Ser294Ala mutated ERα expression construct produces transcriptional suppression of E2 inducible genes. A. Immunoblot analysis of ERα protein levels in MCF levels following transfection with empty vector, exogenous wildtype (WT) ERα or Ser294Ala ERα in the absence (C) or presence (E2) of 10 nM E2 for 6 h. Note the similar degree of ERα downregulation following E2 stimulation relative to basal levels in all three transfection sets. Equal protein loading was confirmed by probing for β-actin. B. Quantitation of gene transcript levels by densitometry of PCR products visualized with ethidium. Levels of three E2 inducible genes (AREG, EGR3, CXCL12) are normalized relative to empty vector control levels (set equal to 1.0) with all gene transcripts levels originally normalized by their respective GAPDH. Error bars represent standard deviation of densitometer quantifications obtained from three biological replicates; asterisks indicate significant reductions ($p<0.05$) in the Ser294Ala inductions relative to E2 stimulated empty vector and WT ERα transfectants as assessed by Student's t-test (two way, unpaired). See Methods for specific gene primers.

FIGURE 2. Phosphorylation of ERα Ser294 is induced by E2, but not EGF, in MCF-7 cells. **A.** MRM/MS assay chromatograms for the phosphorylated and unmodified Ser294 and Ser167 peptides from trypsin-digested ERα immunoprecipitates from MCF-7 cells. The MRM/MS transitions used to quantify the Ser294 peptide, 288-AANLWPSPLMIK-299, were Q1/Q3 670.9/785.5 corresponding to the $[M+2H]^{2+}$ precursor and y7 fragment ion for the unmodified peptide and for the phosphorylated peptide Q1/Q3 710.9/767.4 was used corresponding to the $[M+2H]^{2+}$ precursor and y7-98 fragment ion. The MRM transitions used to quantify the Ser167 peptide, 165-LASTNDKGSMAMESAK-180, were Q1/Q3 547.6/764.3 corresponding to the $[M+3H]^{3+}$ precursor and $y15^{2+}$ for the unmodified peptide and for the phosphorylated peptide Q1/Q3 574.2/755.3 was used corresponding to the $[M+3H]^{3+}$ precursor and $y15^{2+}$-49 fragment ion. MCF-7 cells were treated with 10 nM E2 for 30 min or 8 nM EGF for 10 min. For EGF treatment, cells were serum starved (NS) for 24 h prior to treatment and for E2 cells were grown in charcoal stripped media (CS) for 24 h prior to treatment. **B.** MRM peak areas were used to calculate

the phosphorylated:unmodified peptide area ratio, the relative MRM/MS peak areas of the phosphorylated 167 and 294 peptides normalized to the MRM/MS peak area of the unmodified peptide for each condition in A. Error bars represent the standard deviation of at least 4 biological replicates. And asterisks indicate a significant difference ($p<0.05$) between the treatments and respective controls as assessed by Student's t-test (two way, unpaired). **C.** Western analysis of pSer167 levels induced following E2 and EGF treatments similar to those described in A confirm the concordance of western blot results with the MRM pSer167 induction results shown in B. Ser167 phosphorylation is induced by E2 in CS, but not NS, growth conditions. **D.** Determination of the maximal stoichiometry of Ser294 and Ser167 phosphorylation using SID-MRM. The percent phosphorylation of Ser294 and Ser167 are maximal under E2 and EGF treatment, respectively, which are shown. Cells were grown in serum free conditions for 24 h. Error bars represent the standard of deviation of two independent biological replicates.

FIGURE 3. E2, but not EGF, induces phosphorylation of Ser294 in multiple cells lines. MRM/MS analysis of the induction of Ser294 phosphorylation by E2 and EGF in BT474, MCF7, and T47D cell lines. **A.** In all cell lines E2 induces Ser294 phosphorylation. **B.** EGF stimulation does not induce Ser294 phosphorylation in any cells line. Cells were treated with 8 nM EGF for 10 min or 10 nM E2 for 30 min. For EGF treatment, cells were serum starved (NS) for 24 h prior to treatment and for E2, cells were grown in charcoal stripped media (CS) for 24 h prior to treatment. Error bars represent the standard of deviation of at least 3 biological replicates. Asterisks represent a significant change ($p < 0.05$) as assessed by student t-test (two way, unpaired).

FIGURE 4. ERα hinge domain phosphorylation at Ser294 and Ser305 is suppressed by crosstalk between growth factor and ligand stimulation whereas N-terminal phosphorylation at pSer118 and pSer167 is enhanced. **A.** MCF-7 cells in serum-free conditions were either untreated (CTL), treated with E2 (10 nM) for 30 min, EGF (8 nM) for 14 min, or 10 μM forskolin (Fors) for 14 min. **B.** Western analysis of ER immunoprecipitated from MCF-7 cells either untreated (----), treated with EGF (8 nM) for 20 min, treated with E2 (10 nM) for 20 min (E2), or co-treated with EGF (8 nM) and E2 (10 nM, 2 nM,

0.2 nM) for 20 min. Total ERα served to normalize lane loading. **C.** MRM/MS analysis of immunoprecipitated/trypsin digested ER from MCF7 cells; untreated (CTL), E2 (10 nM), EGF (8 nM), and E2+EGF (10 nM E2, 8 nM EGF) treated samples shown in panel B with the MRM/MS peak area ratio used to determine the induction of Ser294 and Ser167 phosphorylation. % E2 induction of Ser294 and % EGF induction of pSer167 are shown. Asterisk (*) represents a p-value below 0.05 as assessed by student t-test (two way, unpaired).

FIGURE 5. Cyclin-dependent kinases inhibit Ser294 phosphorylation *in vivo* and can phosphorylate Ser294 *in vitro*. **A**. *In vitro* phosphorylation of Ser294 CDKs, including CDK2, CDK4, CDK7, and CDK9 examined by western analysis using pSer294 antibody. **B**. MRM/MS analysis of Ser294 phosphorylation of ER immunoprecipitated from MCF-7 cells treated with 10 nM estradiol (E2) for 30 min or first pre-treated for 1 h with the broad spectrum cyclin-dependent kinase (CDK) inhibitors roscotivine (5 μM and 50 μM) or SNS-032 (1 μM) before E2 treatment. Both inhibitors decrease Ser294 phosphorylation relative to E2 alone (set equal to 100%). Error bars represent the standard deviation for three biological replicates. **C.** Western blot analysis of immunoprecipitated ER also demonstrated a decrease in Ser294 phosphorylation following CDK inhibitor treatment using a pSer294 antibody. Western blot analysis of immunoprecipitated ER using antibodies to pSer118 and pSer104/pSer106 demonstrated that inhibition of CDKs does not reduce their induction by E2. Equal ER loading is confirmed by probing for ERα.

FIGURE 6. A model of ERα phosphorylation under ligand and growth factor stimuli. ERα (purple) consists of an activation function-1 (AF-1), DNA-binding (DBD), hinge, and activation function-2/ligand-binding (LBD/AF-2) domains. Ser118 phosphorylation is induced by both ligand (blue arrow) and growth factor stimulation (green arrow), whereas Ser167 phosphorylation is primarily induced by growth factors (green arrow) though weakly induced by ligand (dashed blue arrow). Kinases shown promoting pSer118 and pSer167 are not meant to exclude other AF-1 phosphorylating candidates; all candidate kinases as well as the indicated kinases promoting pSer305 are described in reference 2 except the ligand stimulation of pSer167 found in reference 27 and results shown in Figure 2C. In the hinge

domain, our study determined that Ser294 is phosphorylated by a cyclin-dependent kinase (CDK) which is exclusively ligand-induced. Ser305 is induced only by growth factors. In contrast to the phosphorylation sites in the AF-1 domain which are co-stimulated by ligand and growth factors, hinge domain phosphorylation at Ser294 and Ser305 is suppressed by co-stimulation with ligand and growth factors (red lines) with the heavier red line to pSer305 relative to the thinner red line to pSer294 indicating the approximately 5 fold greater suppression of pSer305 relative to pSer294 at the co-stimulatory concentration of 10 nM estrogen with 8 nM EGF (see Figure 4A).

Figure 1

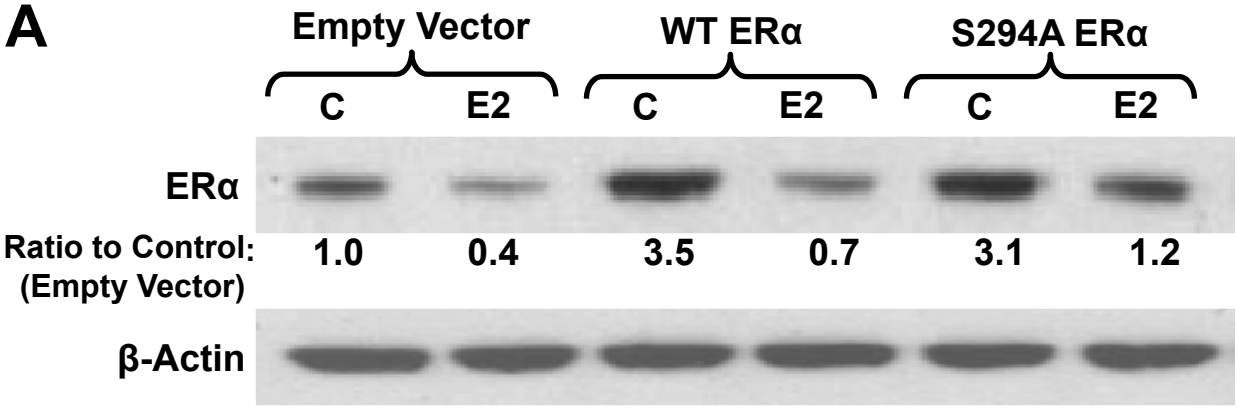
A
Empty Vector
WT ERα
S294A ERα
C
E2
C
E2
C
E2
ERα
Ratio to Control:
(Empty Vector)
1.0
0.4
3.5
0.7
3.1
1.2
β-Actin

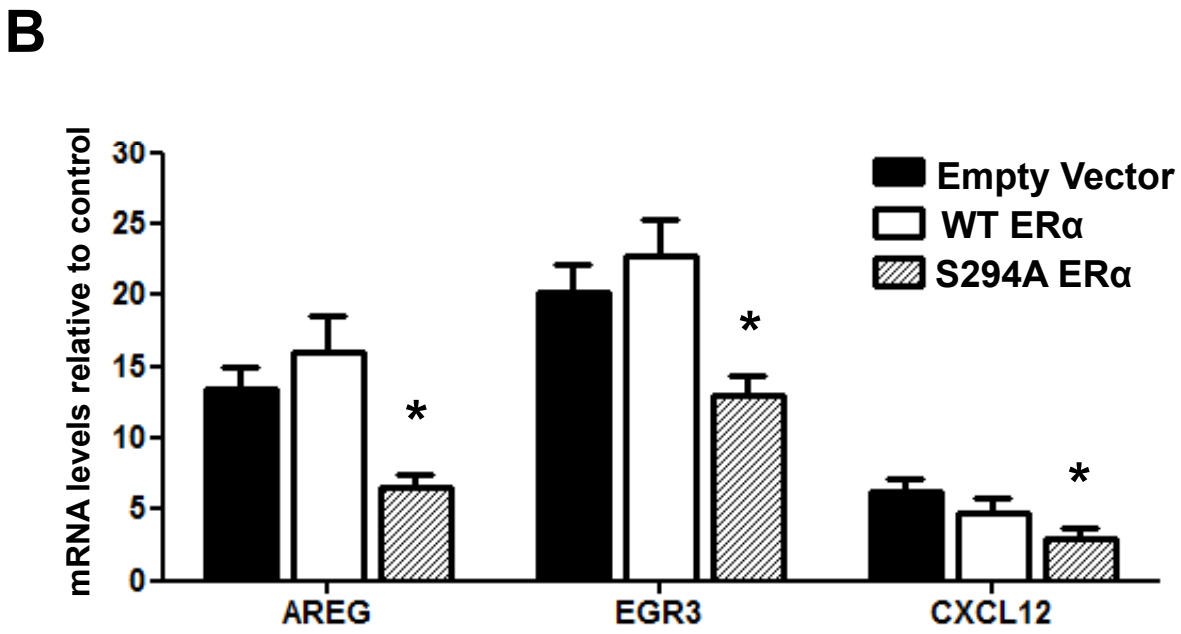
B
mRNA levels relative to control
30
25
20
15
10
5
0
Empty Vector
WT ERα
S294A ERα
*
*
*
AREG
EGR3
CXCL12

Figure 2

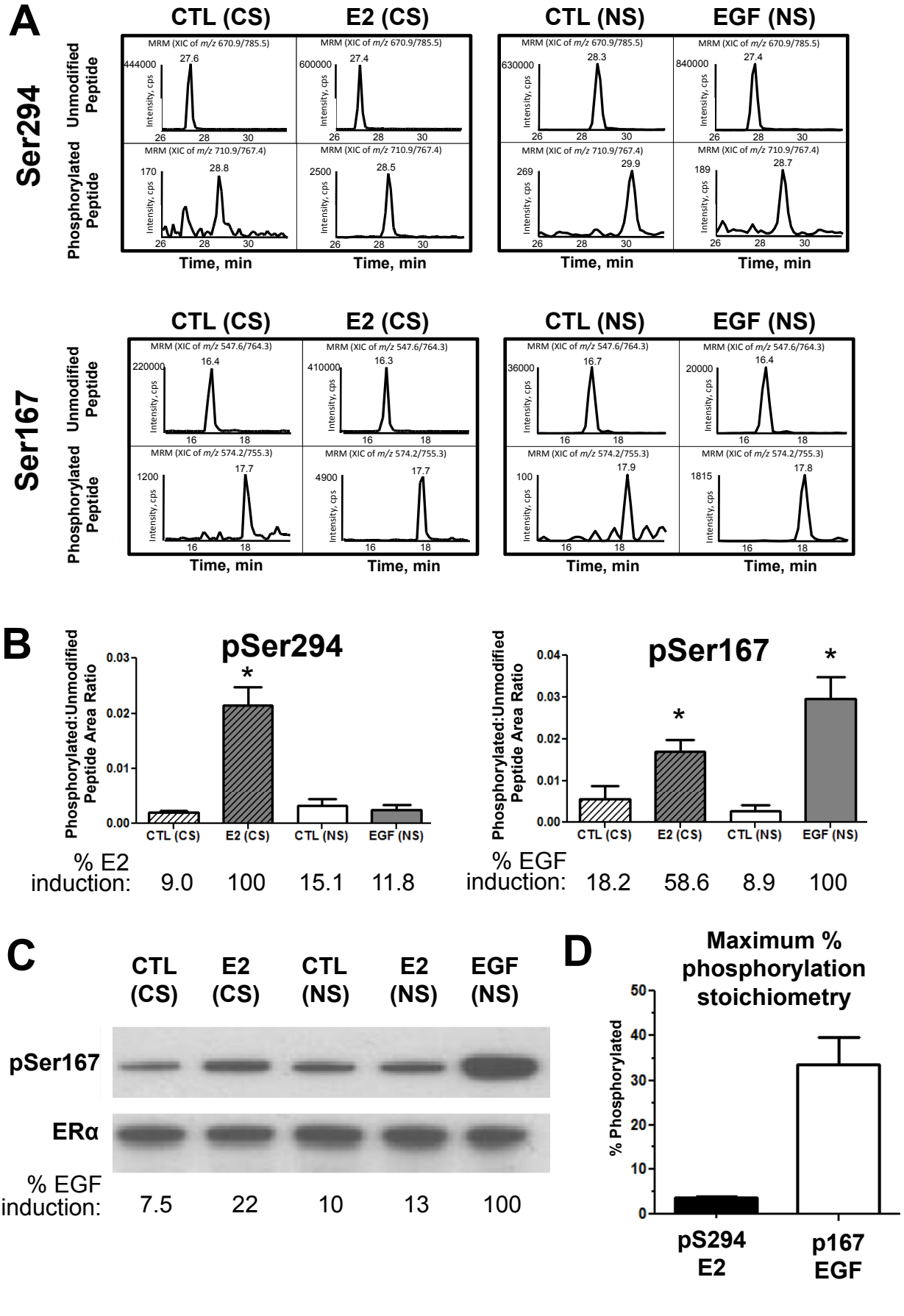
A
CTL (CS)
E2 (CS)
CTL (NS)
EGF (NS)
Ser294
Unmodified Peptide
Phosphorylated Peptide
MRM (XIC of m/z 670.9/785.5)
MRM (XIC of m/z 710.9/767.4)
Intensity, cps
Time, min
Ser167
MRM (XIC of m/z 547.6/764.3)
MRM (XIC of m/z 574.2/755.3)
B
pSer294
pSer167
Phosphorylated:Unmodified Peptide Area Ratio
CTL (CS)
E2 (CS)
CTL (NS)
EGF (NS)
% E2 induction: 9.0 100 15.1 11.8
% EGF induction: 18.2 58.6 8.9 100
C
CTL (CS)
E2 (CS)
CTL (NS)
E2 (NS)
EGF (NS)
pSer167
ERα
% EGF induction: 7.5 22 10 13 100
D
Maximum % phosphorylation stoichiometry
% Phosphorylated
pS294 E2
p167 EGF

Figure 3

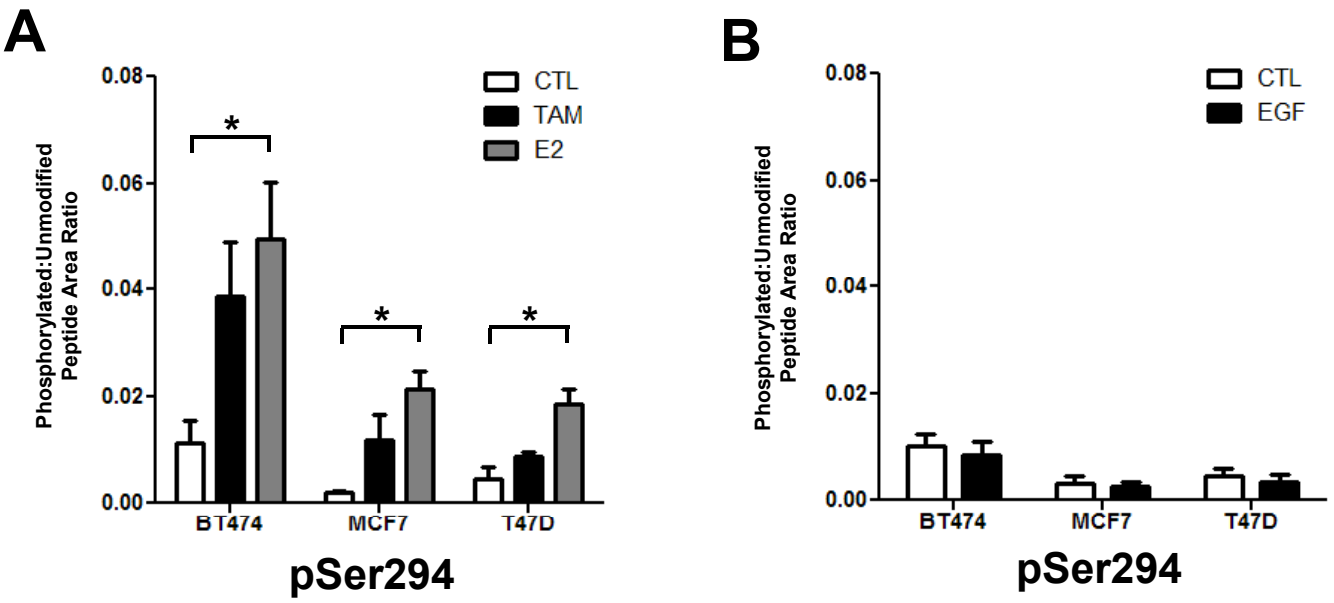
A
0.08
0.06
0.04
0.02
0.00
Phosphorylated:Unmodified Peptide Area Ratio
CTL
TAM
E2
*
*
*
BT474
MCF7
T47D
pSer294
B
0.08
0.06
0.04
0.02
0.00
Phosphorylated:Unmodified Peptide Area Ratio
CTL
EGF
BT474
MCF7
T47D
pSer294

Figure 4

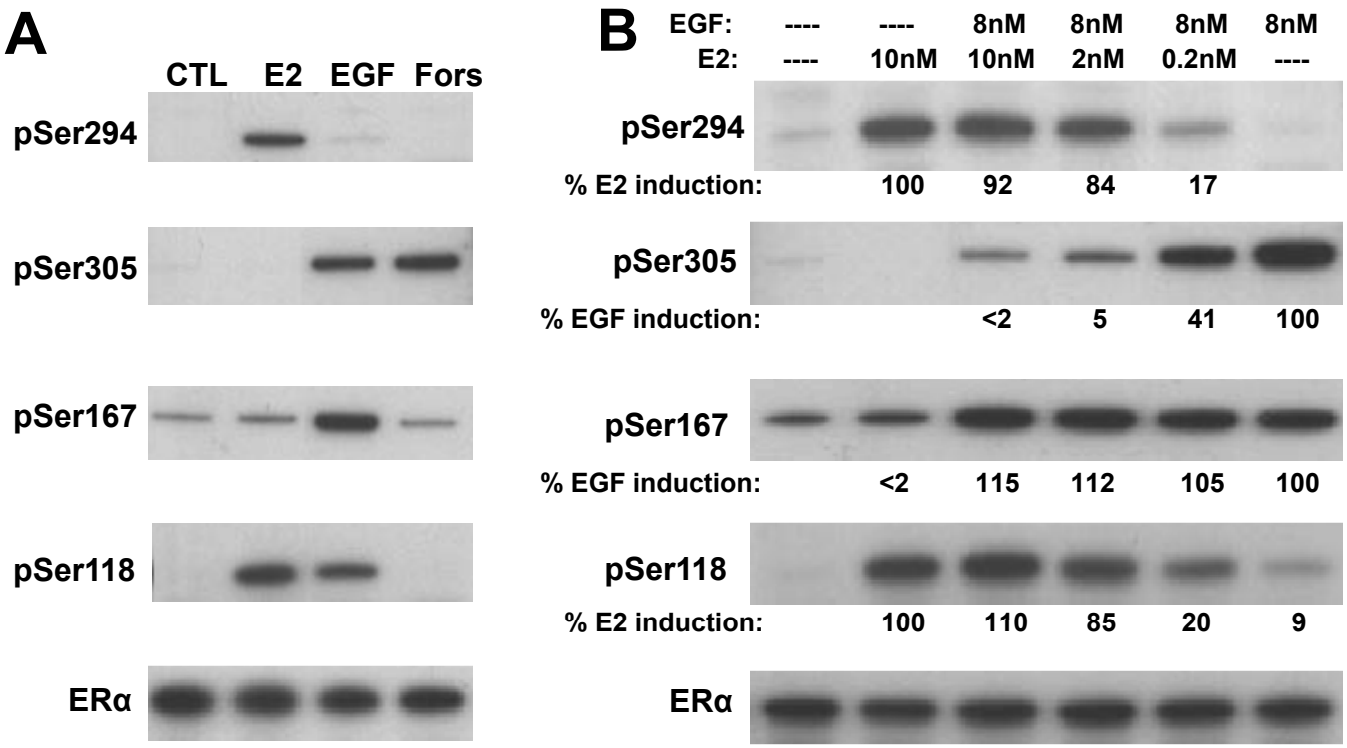
A
CTL
E2
EGF
Fors
pSer294
pSer305
pSer167
pSer118
ERα
B
EGF:
E2:
---- ---- 8nM 8nM 8nM 8nM
---- 10nM 10nM 2nM 0.2nM ----
pSer294
% E2 induction: 100 92 84 17
pSer305
% EGF induction: <2 5 41 100
pSer167
% EGF induction: <2 115 112 105 100
pSer118
% E2 induction: 100 110 85 20 9
ERα

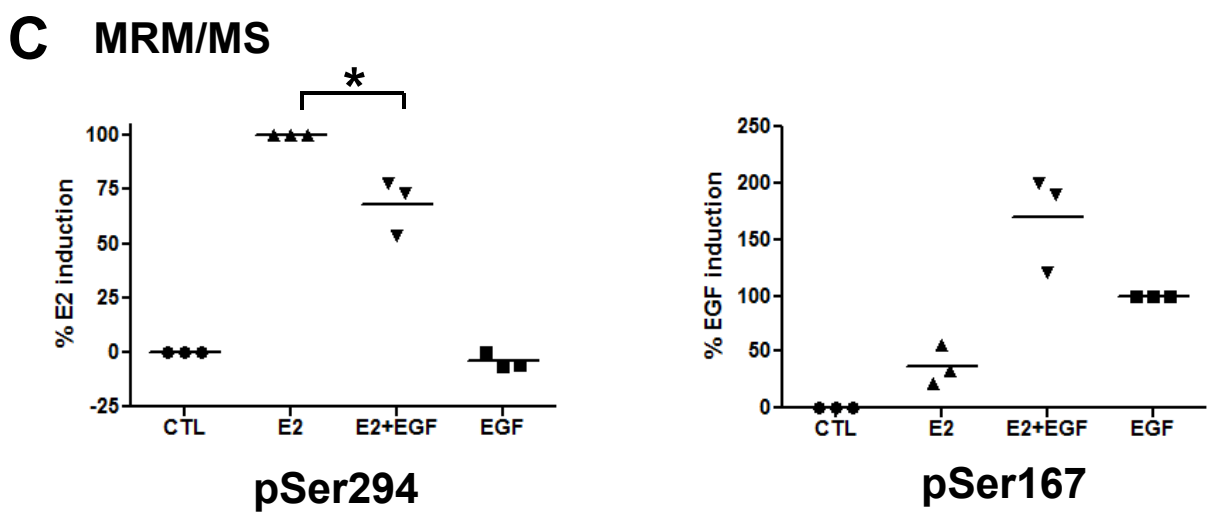
C MRM/MS
*
% E2 induction
100
75
50
25
0
-25
CTL
E2
E2+EGF
EGF
pSer294
% EGF induction
250
200
150
100
50
0
CTL
E2
E2+EGF
EGF
pSer167

Figure 5

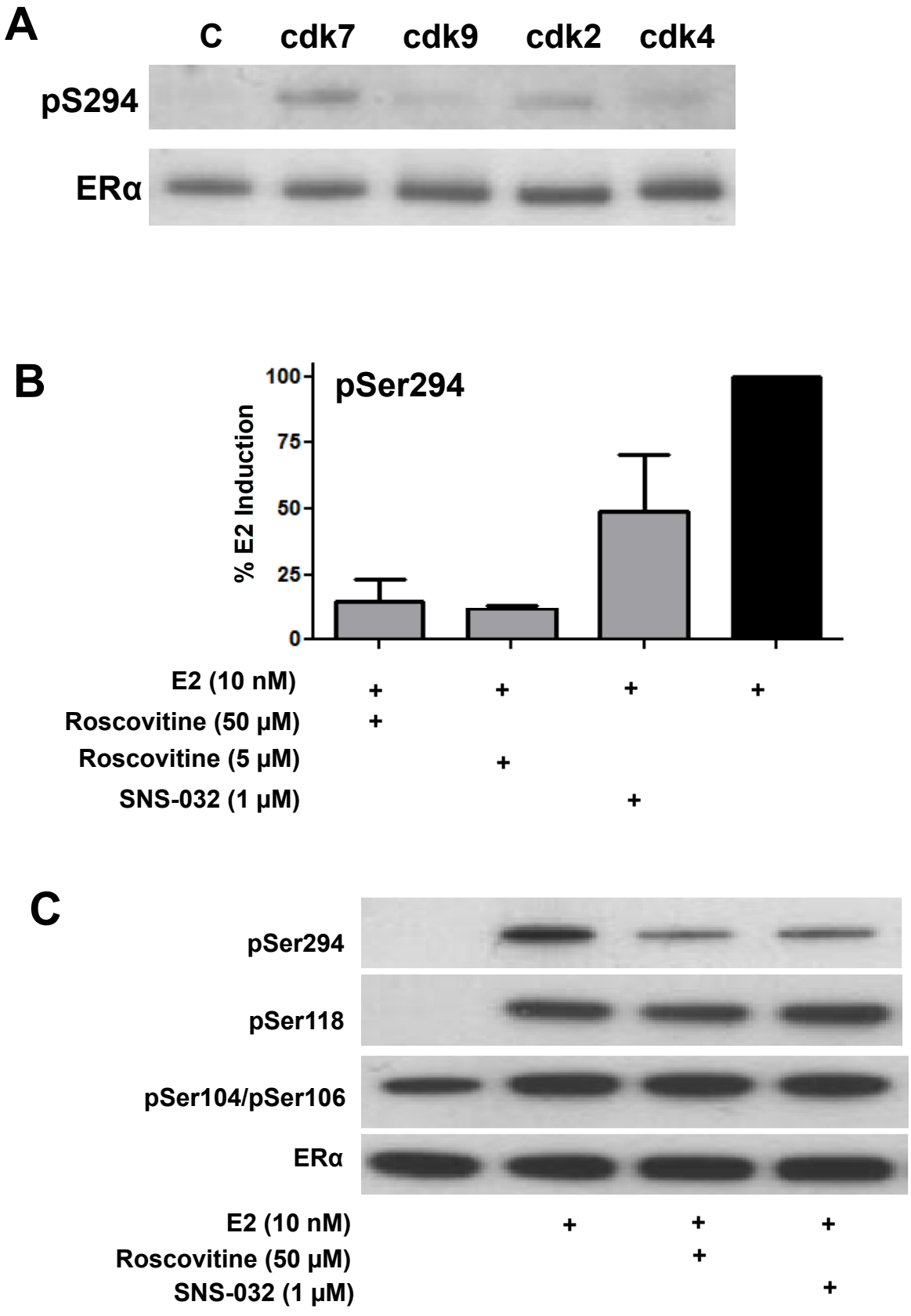
A
C
cdk7
cdk9
cdk2
cdk4
pS294
ERα
B
pSer294
% E2 Induction
100
75
50
25
0
E2 (10 nM)
Roscovitine (50 μM)
Roscovitine (5 μM)
SNS-032 (1 μM)
C
pSer294
pSer118
pSer104/pSer106
ERα
E2 (10 nM)
Roscovitine (50 μM)
SNS-032 (1 μM)

Figure 6

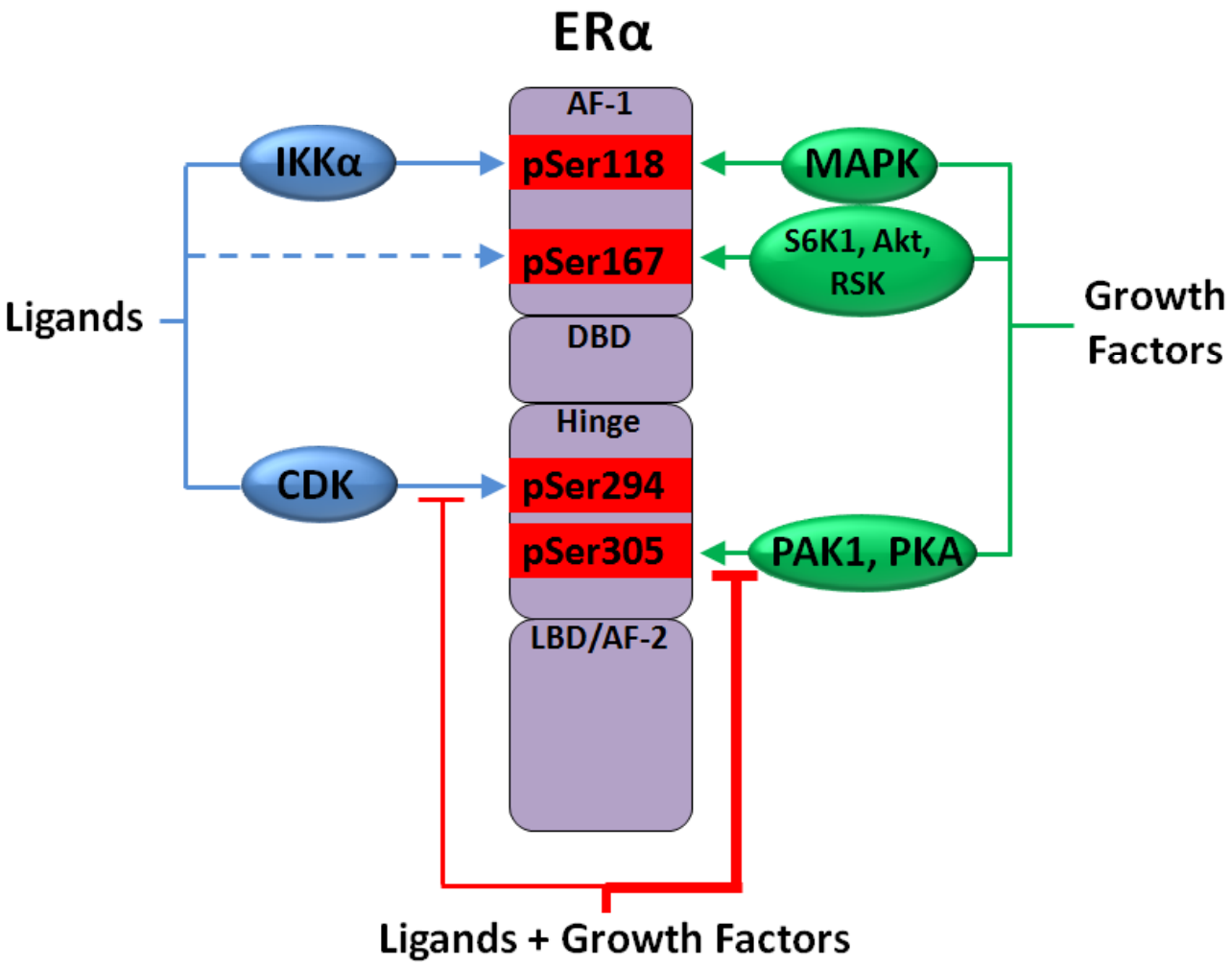
ERα
AF-1
pSer118
pSer167
DBD
Hinge
pSer294
pSer305
LBD/AF-2
IKKα
CDK
MAPK
S6K1, Akt, RSK
PAK1, PKA
Ligands
Growth Factors
Ligands + Growth Factors